MicroRNA-21 maintains hematopoietic stem cell homeostasis through sustaining the nuclear factor-κB signaling pathway in mice

Mengjia Hu, Yukai Lu, Hao Zeng, Zihao Zhang, Shilei Chen, Yan Qi, Yang Xu, Fang Chen, Yong Tang, Mo Chen, Changhong Du, Mingqiang Shen, Fengchao Wang, Yongping Su, Song Wang# and Junping Wang#

[1]State Key Laboratory of Trauma, Burns and Combined Injury, Institute of Combined Injury, Chongqing Engineering Research Center for Nanomedicine, College of Preventive Medicine, Third Military Medical University, Chongqing, China

#SW and JW contributed equally as co-senior authors

 doi:10.3324/haematol.2019.236927

Received: August 30, 2019.

Accepted: January 20, 2020.

Pre-published: January 23, 2020.

Correspondence: *JUNPING WANG* - wangjunping@tmmu.edu.cn

Supplementary Methods

Hematological analysis and irradiation. Hematological analysis and irradiation were conducted as we described[1].

5-fluorouracil (5-FU) treatment. Mice were given a single dose of 5-FU (150 mg/kg; Sigma) by intraperitoneal injection. At each indicated time after injection, mice were sacrificed and their BM cells and LSKs were measured. In another experiment, mice were weekly injected with 5-FU (150 mg/kg) for 3 weeks, and then the survival rates were monitored.

miR-21 agomir and NF-κB inhibitor treatment. Mice were given with 3 doses of miR-21-5p agomir (30mg/kg for each dose; GenePharma, Shanghai, China) on consecutive days by tail intravenous injection. Mismatched oligos (GenePharma Company) was served as negative control (NC) and used at similar doses. For NF-κB inhibition, mice were administrated with a specific NF-κB inhibitor, QNZ (1 mg/kg; MedChem Express, NJ, USA), by intraperitoneal injection.

Transplantation assays. For non-competitive bone marrow transplantation (BMT), 1×10^6 CD45.2$^+$ BM cells from miR-21$^{fl/fl}$ or miR-21$^{\Delta/\Delta}$ mice were transplanted into 10.0 Gy-irradiated CD45.1$^+$ recipients. Sixteen weeks later, 1×10^6 BM cells harvested from primary recipients were transplanted into 10.0 Gy-irradiated secondary CD45.1$^+$ recipients. The survival rates were monitored after transplantations.

For competitive BMT, 5×10^5 CD45.2$^+$ BM cells from miR-21$^{fl/fl}$ or miR-21$^{\Delta/\Delta}$ mice, mixed with 5×10^5 competitor BM cells from CD45.1$^+$ WT mice, were transplanted into 10.0 Gy-irradiated CD45.1$^+$ recipients. Sixteen weeks later, 1×10^6 BM cells harvested from primary recipients were transplanted into 10.0 Gy-irradiated

secondary CD45.1^{+} recipients. In another competitive BMT, 5×10^{5} CD45.2^{+} BM cells from miR-21$^{fl/fl}$;Mx1-Cre^{-} or miR-21$^{fl/fl}$;Mx1-Cre^{+} mice without pIpC treatment, mixed with 5×10^{5} competitor BM cells from CD45.1^{+} WT mice, were transplanted into 10.0 Gy-irradiated CD45.1^{+} recipients. Eight weeks later, all recipients were injected with pIpC. For reciprocal BMT, 1×10^{6} CD45.1^{+} BM cells were transplanted into 10.0 Gy-irradiated CD45.2^{+} miR-21$^{fl/fl}$ or miR-21$^{\Delta/\Delta}$ recipients. At each indicated time after transplantation, PB or BM samples obtained from recipients were analyzed by flow cytometry. The transplantations after lentiviral transduction were performed as described below.

Luciferase reporter assay. The fragment of wild type (WT)-PDCD4 containing the predicted miR-21 binding site, as well as the corresponding mutant (MUT)-PDCD4, were amplified and cloned into the pmirGLO vector (Promega Corporation, Madison, WI, USA). After that, miR-21 mimic or miRNA-neagive control (miR-NC), together with WT-PDCD4 or MUT-PDCD4, were co-transfected into 293T cells using lipofectamine 3000 (Invitrogen, Carlsbad, CA, USA). Forty-eight hours later, the relative luciferase activity was measured.

Quantitative RT-PCR (qRT-PCR). RNA was extracted from freshly sorted cells using the RNAqueous kit (Ambion, Darmstadt, Germany). The expression of mRNAs or miR-21-5p was detected as we described[2,3]. The primers sequences are provided in Supplementary Table 2.

Western blotting. Western blotting was performed as we reported[4]. The following antibodies were used: anti-PDCD4 (Abcam, Cambridge, UK), anti-Spry1 (Novus, Littleton, CO, USA), anti-Spry2 (Abcam), anti-PTEN (Abcam), anti-p-p65 (Cell Signaling Technology, Danvers, MA, USA), anti-p65 (Cell Signaling Technology)

and anti-β-actin (Cell Signaling Technology). The detailed information for antibodies used for western blotting analysis is provided in Supplementary Table S1.

Immunofluorescence microscopy. Freshly sorted LSKs were placed on Poly-L-lysine coating slides. After fixation, permeabilization and blocking, samples were stained with anti-PDCD4 (Abcam), anti-p-p65 (Cell Signaling Technology) and γ-H2AX^{S139} (Abcam) antibodies. Then, some samples were incubated with secondary antibodies (Invitrogen) and 4',6-diamidino-2-phenylindole (DAPI, Sigma), and imaged using a Zeiss LSM800 confocal microscope (Carl Zeiss, Jena, Germany). The detailed information for antibodies used for western blotting analysis is provided in Supplementary Table S1.

Supplementary References

1. Xu Y, Wang S, Shen M, et al. hGH promotes megakaryocyte differentiation and exerts a complementary effect with c-Mpl ligands on thrombopoiesis. Blood. 2014;123(14):2250-2260.
2. Long S, Zhao N, Ge L, et al. MiR-21 ameliorates age-associated skin wound healing defects in mice. J Gene Med. 2018;20(6):e3022.
3. Zeng H, Hu M, Lu Y, et al. MicroRNA 34a promotes ionizing radiation-induced DNA damage repair in murine hematopoietic stem cells. FASEB J. 2019;33(7):8138-8147.
4. Hu M, Zeng H, Chen S, et al. SRC-3 is involved in maintaining hematopoietic stem cell quiescence by regulation of mitochondrial metabolism in mice. Blood. 2018;132(9):911-923.

Supplementary Figure S1

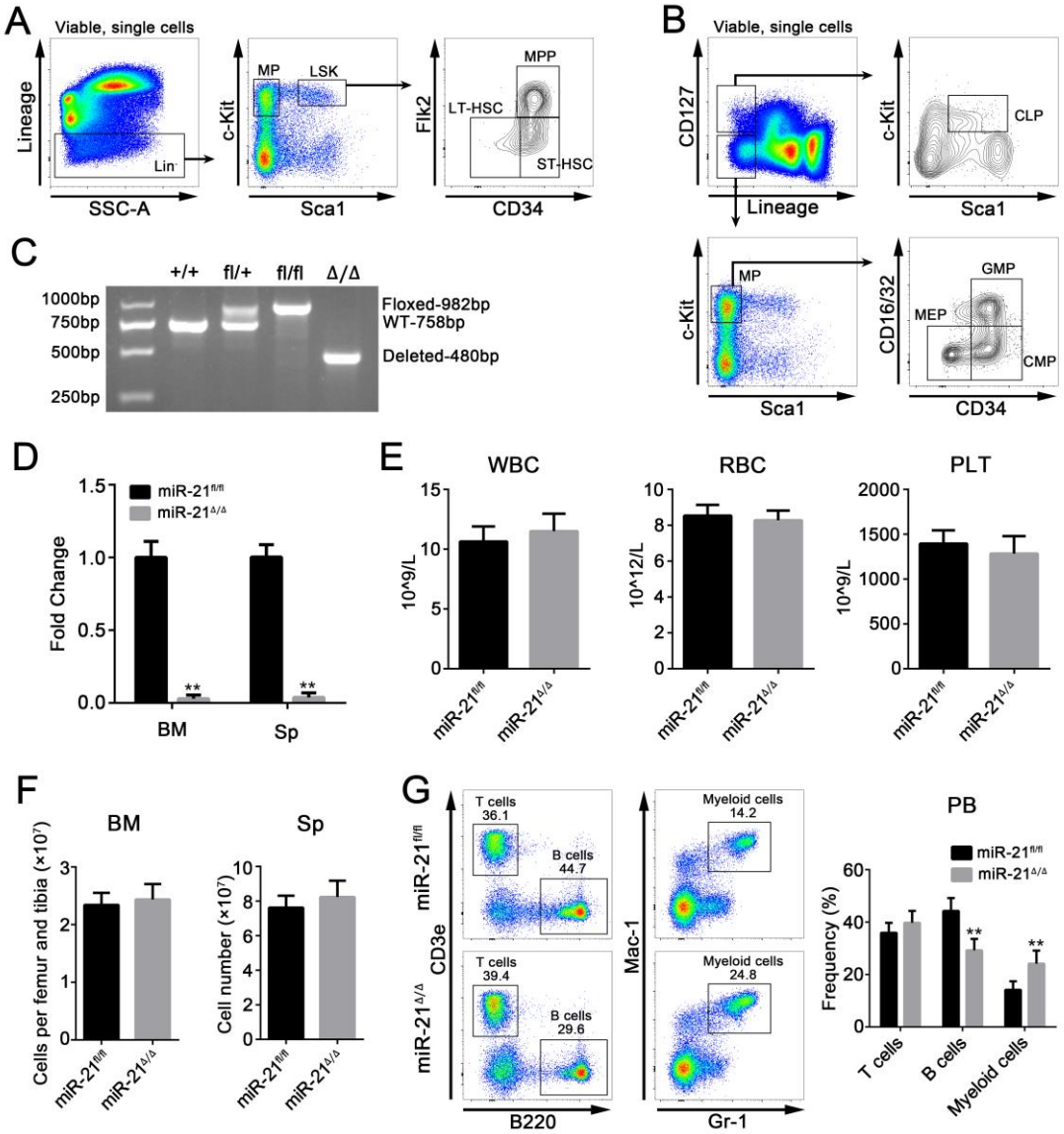

Supplementary Figure S1. The conditional deletion of miR-21 disturbs normal hematopoiesis in mice. (**A**) Flow cytometric gating strategies for identifying Lin$^-$ cells, MP (Lin$^-$ Sca1$^-$ c-Kit$^+$), LSK (Lin$^-$ Sca1$^+$ c-Kit$^+$), LT-HSC (Lin$^-$ Sca1$^+$ c-Kit$^+$ CD34$^-$ Flk2$^-$), ST-HSC (Lin$^-$ Sca1$^+$ c-Kit$^+$ CD34$^+$ Flk2$^-$) and MPP (Lin$^-$ Sca1$^+$ c-Kit$^+$ CD34$^+$ Flk2$^+$) in the BM. (**B**) Flow cytometric gating strategies for identifying CMP (Lin$^-$ CD127$^-$ Sca1$^-$ c-Kit$^+$ CD16/32$^-$ CD34$^+$), GMP (Lin$^-$ CD127$^-$ Sca1$^-$ c-Kit$^+$ CD16/32$^+$ CD34$^+$), MEP (Lin$^-$ CD127$^-$ Sca1$^-$ c-Kit$^+$ CD16/32$^-$ CD34$^-$) and CLP (Lin$^-$

CD127^{+} Sca1^{+} c-Kit^{+}) in the BM. (**C**). Genotyping for the conditional deletion of miR-21. Primers P1 and P2 were used to amplify wild-type (WT) band (758 bp), floxed band (982 bp) and deleted band (480 bp). (**D**) QRT-PCR analysis of miR-21 expression in the BM and spleen (Sp) from miR-21$^{fl/fl}$ and miR-21$^{\Delta/\Delta}$ mice (n = 3 mice per group). (**E**) The counts of white blood cell (WBC), red blood cell (RBC) and platelet (PLT) in the peripheral blood (PB) of miR-21$^{fl/fl}$ and miR-21$^{\Delta/\Delta}$ mice (n = 8 mice per group). (**F**) BM and spleen (Sp) cell numbers in miR-21$^{fl/fl}$ and miR-21$^{\Delta/\Delta}$ mice (n = 6 mice per group). (**G**) Flow cytometric analysis of the percentages of T cells (CD3e^{+}), B cells (B220^{+}) and myeloid cells (Gr-1^{+} and Mac-1^{+}) in the PB of miR-21$^{fl/fl}$ and miR-21$^{\Delta/\Delta}$ mice (n = 6 mice per group). All data are shown as means ± SD. **P < 0.01.

Supplementary Figure S2

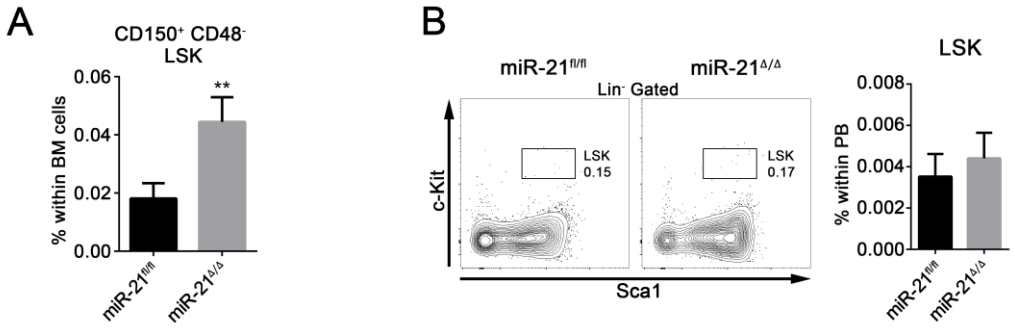

Supplementary Figure S2. Loss of miR-21 leads to an obvious increase in HSC percentage in the BM but not the peripheral blood of mice. (**A**) Flow cytometric analysis of the percentage of $CD150^{+}$ $CD48^{-}$ LSKs in miR-$21^{fl/fl}$ and miR-$21^{\Delta/\Delta}$ BM (n = 6 mice per group). (**B**) Flow cytometric analysis of the percentage of LSKs in the peripheral blood (PB) of miR-$21^{fl/fl}$ and miR-$21^{\Delta/\Delta}$ mice (n = 6 mice per group). All data are shown as means ± SD. **P < 0.01.

Supplementary Figure S3

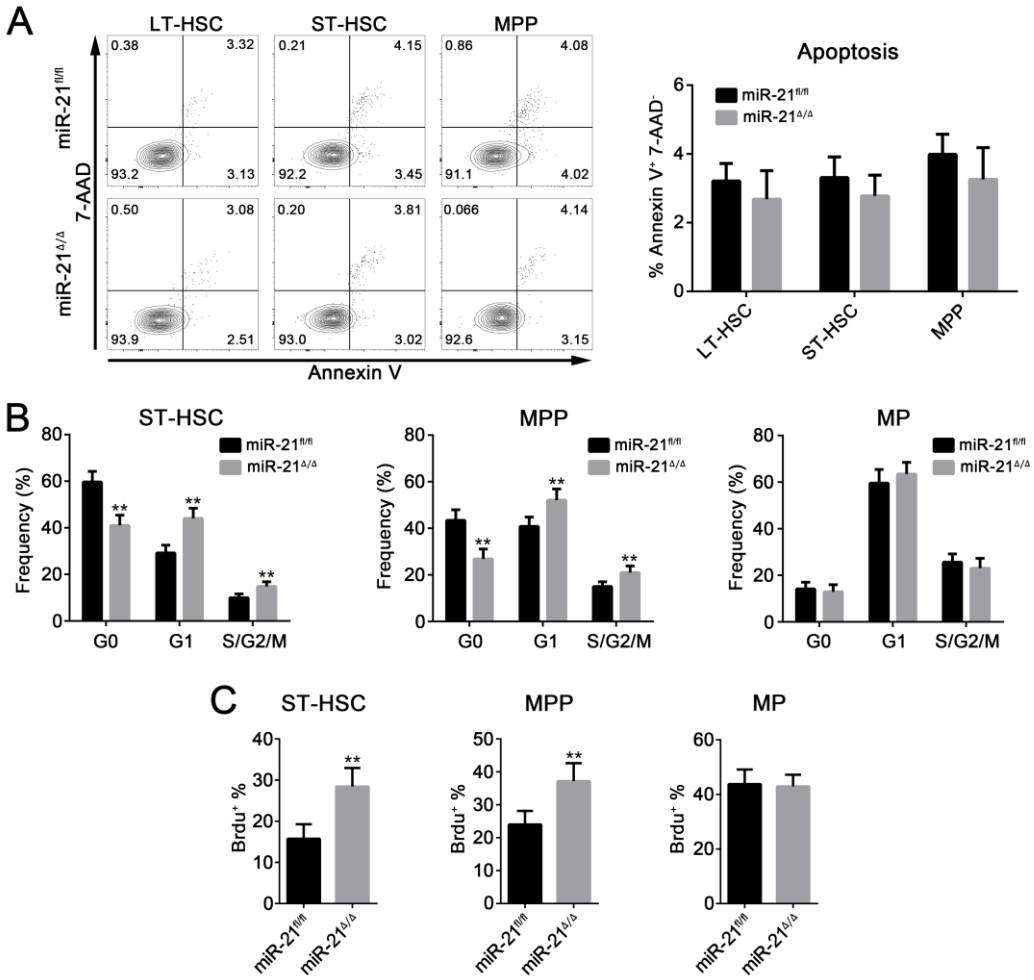

Supplementary Figure S3. The effects of miR-21 deficiency on HSPC apoptosis, quiescence and proliferation. (**A**) Flow cytometric analysis of the percentage of apoptotic cells (Annexin V^+ and 7-AAD^-) in LT-HSC, ST-HSC and MPP from the BM of miR-$21^{fl/fl}$ and miR-$21^{\Delta/\Delta}$ mice (n = 6 mice per group). (**B**) Cell cycle analysis of ST-HSC, MPP and MP in the BM of miR-$21^{fl/fl}$ and miR-$21^{\Delta/\Delta}$ mice (n = 6 mice per group). (**C**) Flow cytometric analysis of the BrdU incorporation in ST-HSC, MPP and MP from miR-$21^{fl/fl}$ and miR-$21^{\Delta/\Delta}$ BM (n = 6 mice per group). All data are shown as means ± SD. **P < 0.01.

Supplementary Figure S4

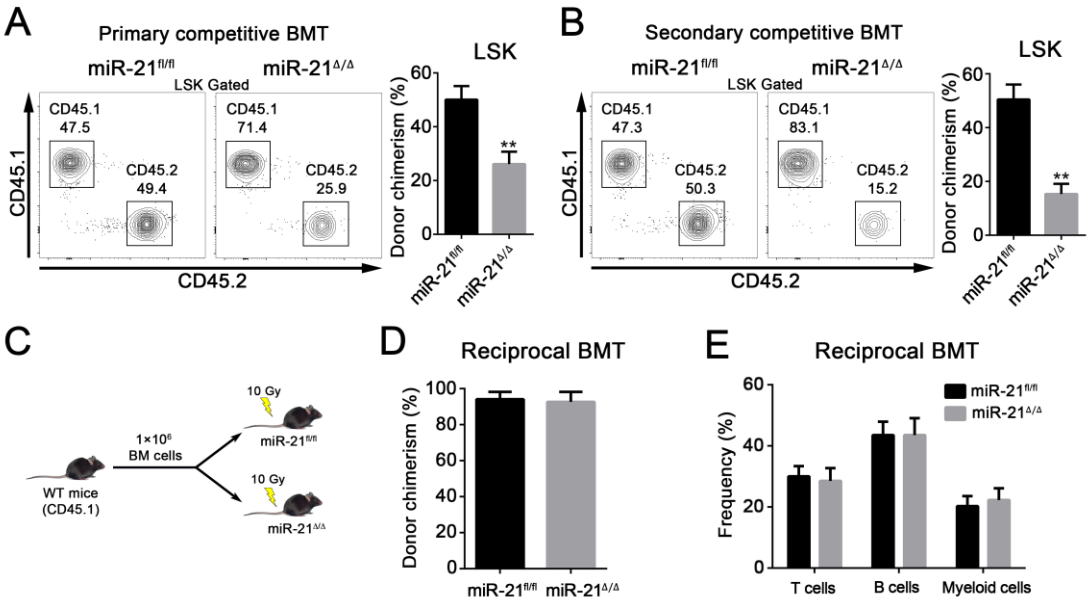

Supplementary Figure S4. miR-21 deficiency intrinsically compromises HSC function in long-term reconstitution. (**A, B**) The chimerism of LSKs in CD45.1^{+} recipients' BM at 16 weeks after (**A**) primary and (**B**) secondary competitive BMT (n = 8 mice per group). (**C-E**) CD45.1^{+} BM cells were transplanted into 10.0 Gy-irradiated CD45.2^{+} miR-21$^{fl/fl}$ or miR-21$^{\Delta/\Delta}$ recipients. At 16 weeks after transplantation, the (**D**) percentage and (**E**) lineage distribution of CD45.1^{+} donor-derived cells in the PB of miR-21$^{fl/fl}$ and miR-21$^{\Delta/\Delta}$ recipients were analyzed by flow cytometry (n = 8 mice per group). The schematic diagram of reciprocal BMT assay is shown in the left panel. All data are shown as means ± SD. **P < 0.01.

Supplementary Figure S5

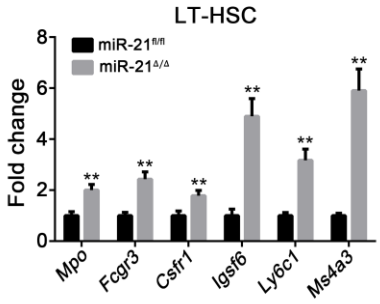

Supplementary Figure S5. Loss of miR-21 results in increased expression of myeloid differentiation-associated genes in HSCs. QRT-PCR analysis of the relative expression of myeloid differentiation-associated genes (including *Mpo*, *Fcgr3*, *Csf1r*, *Igsf6*, *Ly6c1* and *Ms4a3*) in LT-HSCs from miR-21$^{fl/fl}$ and miR-21$^{\Delta/\Delta}$ BM (n = 3 mice per group). Data are showed as mean ± SD. All data are shown as means ± SD. **P < 0.01.

Supplementary Figure S6

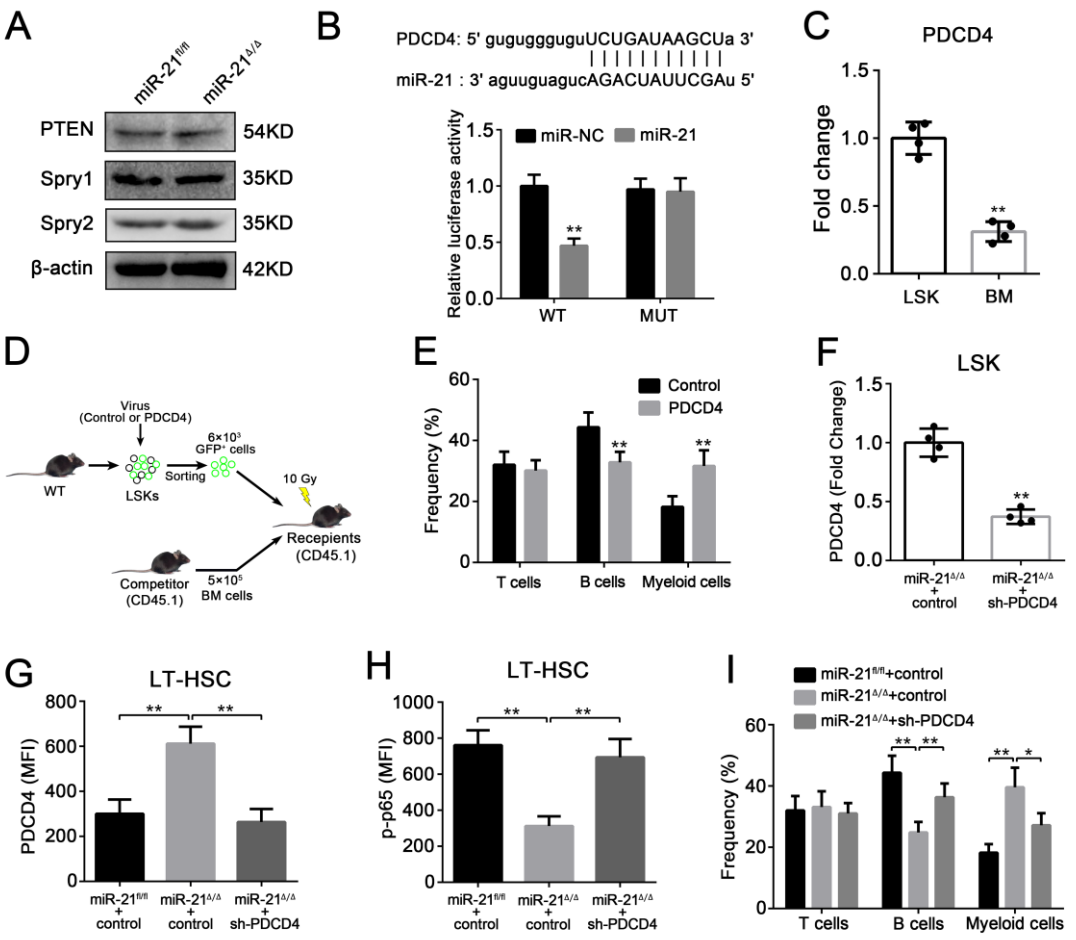

Supplementary Figure S6. The upregulation of PDCD4 is responsible for the defects in miR-21-null HSCs. (**A**) Western blot analysis of the expression of PTEN, Spry1 and Spry2 in miR-21$^{fl/fl}$ and miR-21$^{\Delta/\Delta}$ LSKs (n = 5 mice per group). (B) 293T cells were co-transfected with WT-PDCD4 (3'UTR) or MUT-PDCD4 (3'UTR) and miR-21 or miR-NC, and then the relative luciferase activity was detected. (**C**) QRT-PCR analysis of the relative PDCD4 expression in LSKs and BM cells from normal 8-week-old WT mice (n = 4 mice per group). (**D**) Schematic diagram of lentiviral transduction of PDCD4 and competitive transplantation. (**E**) The lineage distribution of CD45.2^{+} donor-derived cells in recipients' PB 12 weeks after PDCD4 overexpression and competitive transplantation (n = 6 mice per group). (**F**) QRT-PCR

analysis of the relative PDCD4 expression in miR-21$^{\Delta/\Delta}$ LSKs after transducted with control or sh-PDCD4 (n = 4 mice per group). (**G-I**) CD45.2^{+} miR-21$^{fl/fl}$ or miR-21$^{\Delta/\Delta}$ LSKs transduced with control or sh-PDCD4, mixed with CD45.1^{+} competitor BM cells, were transplantated into 10.0 Gy-irradiated CD45.1^{+} recipients. At 12 weeks after transplantation, the expression of (**G**) PDCD4 and (**H**) p-p65 in CD45.2^{+} donor-derived LT-HSCs from recipients' BM, and (**I**) the lineage distribution of CD45.2^{+} donor-derived cells in recipients' PB were detected by flow cytometry (n = 6 mice per group). All data are shown as means ± SD. *P < 0.05, **P < 0.01.

Supplementary Figure S7

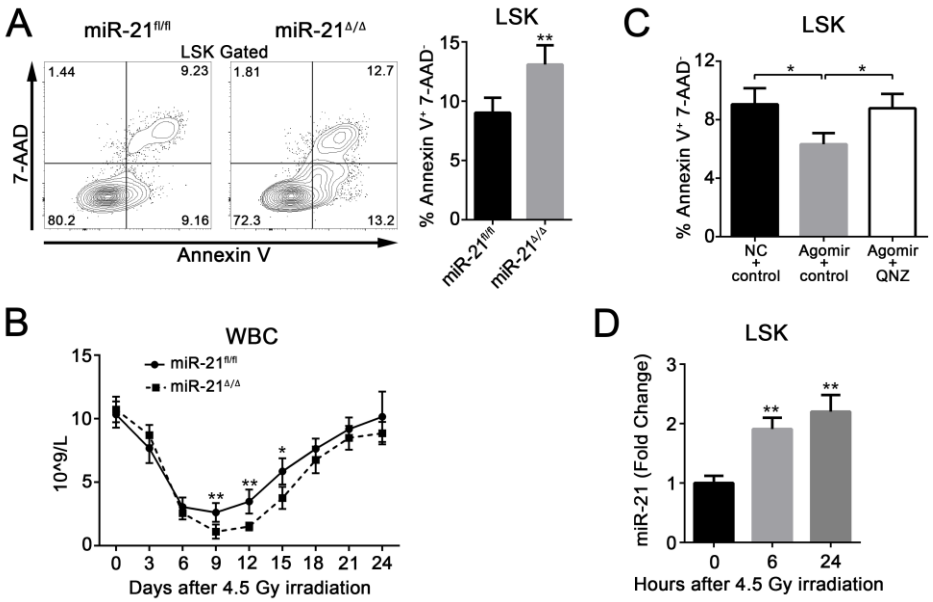

Supplementary Figure S7. miR-21 is involved in protecting HSCs from irradiation-induced damage. (**A**) Flow cytometric analysis of the percentage of apoptotic cells (Annexin V^+ and 7-AAD^-) in LSKs from the BM of miR-$21^{fl/fl}$ and miR-$21^{\Delta/\Delta}$ mice 24 hours after 6.0 Gy TBI (n = 6 mice per group). (**B**) WBC count in the PB of miR-$21^{fl/fl}$ and miR-$21^{\Delta/\Delta}$ mice after 4.5 Gy TBI (n = 6 mice per group). (**C**) Normal WT mice were treated with 3 doses of miR-21 agomir or negative control (NC) on consecutive days by tail intravenous injection. Twenty-one hours after last injection, mice were intraperitoneally injected with one dose of QNZ or control. Three hours later, mice were subjected to 6.0 Gy TBI. The percentage of apoptotic cells in LSKs from these mice was detected 24 hours after irradiation by flow cytometry (n = 6 mice per group). (D) The relative expression of miR-21 in LSKs from normal WT mice at 0, 6 and 24 hours after 4.5 Gy TBI (n = 4 mice per group). The relative miR-21 expression was compared with that in 0 hour group. All data are shown as means ± SD. *P < 0.05, **P < 0.01.

Supplementary Table S1

Antibodies used in flow cytometry, immunofluorescence and western blotting

Antibody	Origin	Cat. No	Assay
V450-Lineage	eBioscience	88-7770-72	FC
FITC-Lineage	eBioscience	22-7770-72	FC
APC-eFluor780-c-Kit	eBioscience	47-1171-82	FC
Pecy7-c-Kit	eBioscience	25-1171-82	FC
Percp-cy5.5-Sca1	eBioscience	45-5981-82	FC
APC-Sca1	Biolegend	108112	FC
PE-CD135	eBioscience	17-1351-82	FC
APC-CD135	Biolegend	135310	FC
eFluor660-CD34	eBioscience	50-0341-82	FC
FITC-CD34	eBioscience	11-0341-82	FC
Alexa Fluor 700-CD34	eBioscience	56-0341-82	FC
PE-CD150	Biolegend	306308	FC
APC-CD48	eBioscience	17-0481-82	FC
PE-B220	eBioscience	12-0452-82	FC
Apccy7-CD3e	eBioscience	47-0031-82	FC
FITC-Gr-1	eBioscience	11-5931-82	FC
APC-Gr-1	Biolegend	108412	FC
Percp-cy5.5-CD11b	eBioscience	45-0112-82	FC
V450-CD45.1	eBioscience	48-0453-82	FC
PE-CD45.1	eBioscience	12-0453-82	FC
Pecy7-CD45.2	eBioscience	25-0454-82	FC
APC-CD45.2	eBioscience	17-0454-82	FC
PE-CD127	eBioscience	12-1271-82	FC
V450-CD16/32	eBioscience	48-0161-82	FC
BV510-Annexin V	Biolegend	640937	FC
FITC-Brdu	BD Pharmingen	559619	FC
Pecy7-Ki67	eBioscience	25-5698-82	FC
eFluor506-Ki67	eBioscience	69-5698-82	FC
PDCD4	Abcam	ab79405	FC, WB, IF
Spry1	Novus	NBP1-51918	WB
Spry2	Abcam	ab85670	WB
PTEN	Abcam	ab32199	WB
p-p65	Cell Signaling Technology	3033S	FC, WB, IF
p65	Cell Signaling Technology	8242s	WB
β-actin	Abcam	ab8227	WB
γ-H2AX (S139)	Abcam	ab26350	FC, IF
Goat anti-Rabbit IgG (H+L) Cross-Adsorbed Secondary Antibody, FITC	Invitrogen	F-2765	FC, IF
Goat anti-Rabbit IgG (H+L) Highly Cross-Adsorbed Secondary Antibody, Alexa Fluor 594	Invitrogen	A-11037	FC, IF

FC, flow cytometry; WB, western blot; IF, immunofluorescence.

Supplementary Table S2

Primers for mRNA expression analysis

Gene	Forward primer (5' - 3')	Reverse primer (5' - 3')
Cdkn1a	AATCCTGGTGATGTCCGACC	TTGCAGAAGACCAATCTGCG
Cdkn1b	TATGGAAGAAGCGAGTCAGC	GCGAAGAAGAATCTTCTGCAG
Ccne1	CCGTCTTGAATTGGGGCAATA	GAGCTTATAGACTTCGCACACC
Ccne2	TCAGCCCTTGCATTATCATTGAA	CCAGCTTAAATCTGGCAGAGG
Ccna2	TGGATGGCAGTTTTGAATCACC	CCCTAAGGTACGTGTGAATGTC
Cdk6	TGGACATCATTGGACTCCCAG	TCGATGGGTTGAGCAGATTTG
Egr1	TATGAGCACCTGACCACAGAG	GCTGGGATAACTCGTCTCCA
Tnf	CTGAACTTCGGGGTGATCGG	GGCTTGTCACTCGAATTTTGAGA
Birc3	TGTGTCAGAAAGGAGTCTGGC	GTTGGCTGGATTCAAAGTCTGT
Nr4a2	GTGTTCAGGCGCAGTATGG	TGTATTCTCCCGAAGAGTGGTAA
Tnfaip3	ACTGGAATGACGAATGGGACA	CAGGGAATTGTACTGAAGTCCAC
Nfkbia	CGAGACTTTCGAGGAAATACCC	GTCTGCGTCAAGACTGCTACA
Csf1r	TGTCATCGAGCCTAGTGGC	GGTCCAAGGTCCAGTAGGG
Fcgr3	CAGAATGCACACTCTGGAAGC	GGGTCCCTTCGCACATCAG
Mpo	AGGGCCGCTGATTATCTACAT	CTCACGTCCTGATAGGCACA
Ly6c1	TCAAAGAAGGAAACTAAAGACCCG	AGCTCAGGCTGAACAGAAGCAC
Igsf6	CCTGATCCTTTTCCAAGTCGG	ACCGTAGTCCACTTCTAGGTAAC
Ms4a3	AGCTGTCCGTGACCATTTCTA	GGAGGTGAAGTAATTGCCTCTC
Pdcd4	AAAGACGACTGCGGAAAAATTCA	CTTCTAACCGCTTCACTTCCATT
Ier3	TCTCCTGTTCGCCATCATCTTC	CAGAAATGGGCTCAGGTGTCA
Gadd45b	TTGACATCGTCCGGGTATCAG	GTCTCGGGCTTCGGTTGTG
Xrcc5	GACTTGCGGCAATACATGTTTTC	AAGCTCATGGAATCAATCAGATCA
Gapdh	CCTCGTCCCGTAGACAAAATG	TCTCCACTTTGCCACTGCAA

Supplementary Table S3

The differentially expressed genes between miR-21$^{fl/fl}$ and miR-21$^{\Delta/\Delta}$ LSKs (uploaded as separate excel file).